Search for Higgs Boson Pair Production in the $bblvlv$ Final States

Zhe Yang

on behalf of the analysis team

Physics Motivations

- HH process is crucial for determining the self-coupling terms that would describe the shape of the Higgs potential
  - ggF mode is studied in current paper (VBF studies are also ongoing in the group)
- Can probe BSM like 2 Higgs Doublet Model (2HDM) which extends the SM sector and predicts a scalar heavy Higgs decaying into SM HH
- $bblvlv$ final states
  - relatively large branch ratio including $bbWW$, $bb\tau\tau$ and $bbZZ$ channels

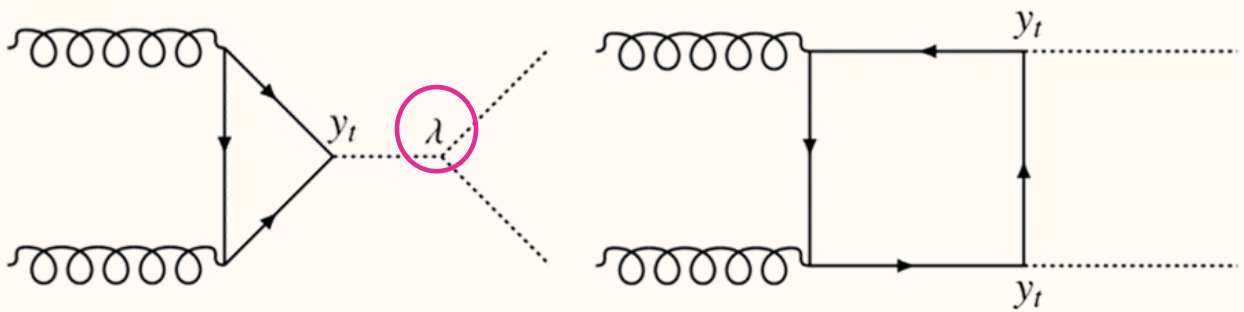

non-resonant

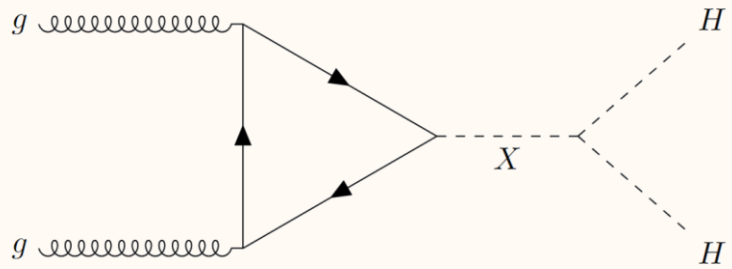

resonant

HH Decay Channels in $bbll$

- multiple HH decay channels contribute to $bbll + MET$ final states ($l = e, \mu$)

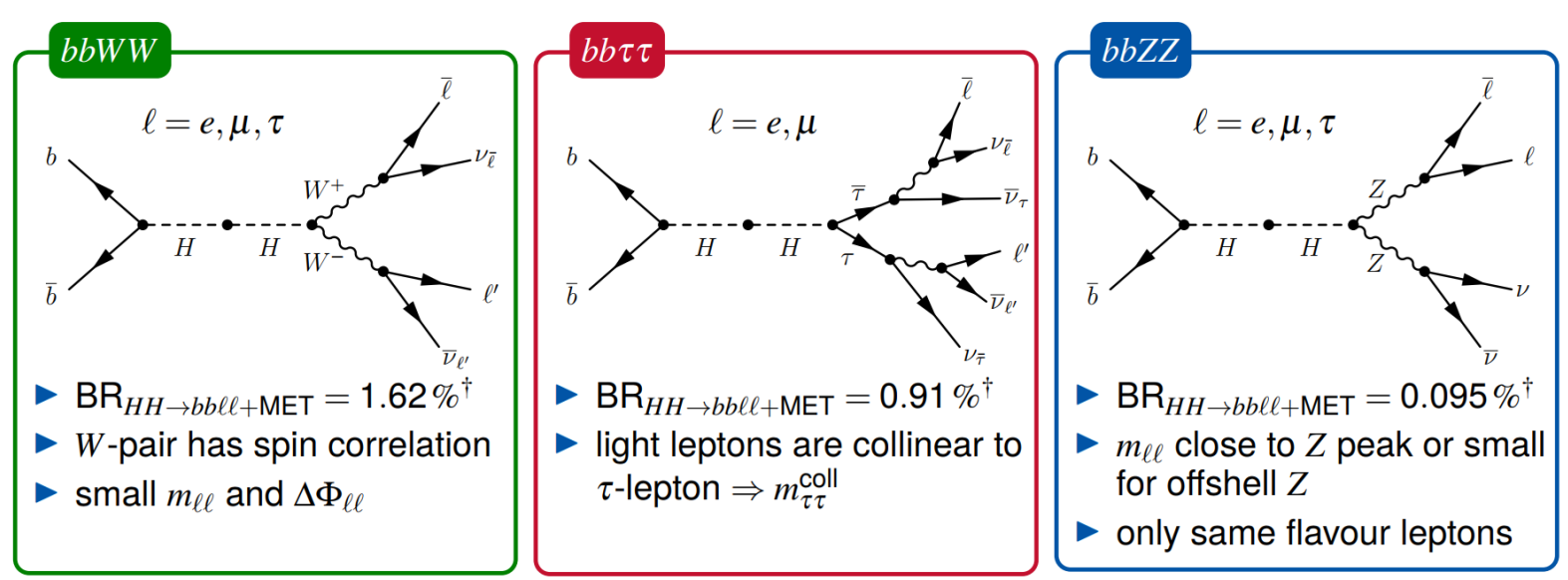

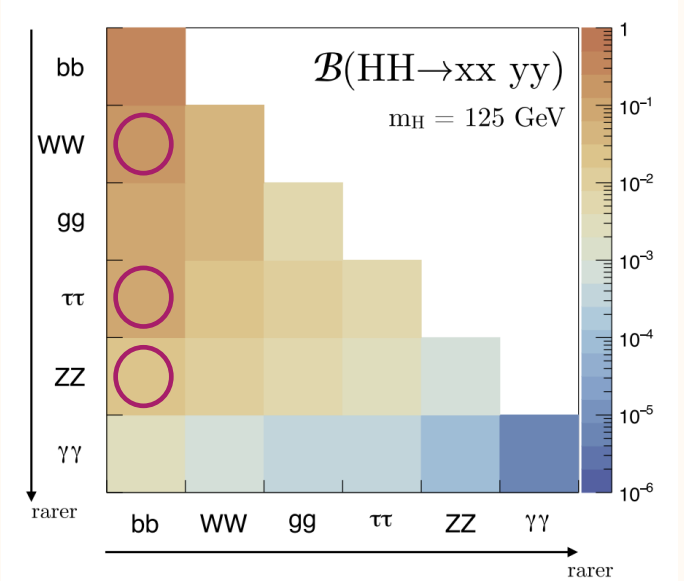

- investigated HH decay channels: bbWW + bb$\tau\tau$ + bbZZ
- unique challenge due to multiple signals with different kinematic properties

Overview of Analysis Methodology

- Signal signature
  - 2 b-tagged jets (DL1r, 77%WP) + opposite charge lepton pair
- Top and Zll estimated in dedicated CR
- Fake (leptons) estimated with MC-driven methods so far
  - plan to use the data-driven OS-SS method to estimate (used in the WWbb paper)
- MVA-based analysis
  - likelihood fit to the MVA scores in two SRs and CR
  - multiple MVA strategy used for different purpose

Data and MC Samples

- Data
  - $139\ fb^{-1}$ collected during the Run 2
- Signals
  - non-resonant ggF [Powheg + Pythia 8] → 3 channels at $\kappa_\lambda = 1\ or\ 10$
  - resonant ggF [MadGraph + Herwig 7] → 8 mass points ranging from 251 to 1000GeV
- Backgrounds
  - $t\bar{t}$ and single top [Powheg + Pythia 8]
  - $t\bar{t}V$ [MadGraph + Pythia 8]
  - $V + jets\ \&\ VV$ [Sherpa]
  - single-$Higgs$ [Powheg + Pythia 8]
  - fake → currently estimated with top, W+jets and some other MC samples (estimation from data-driven OS-SS fake method to be used next)

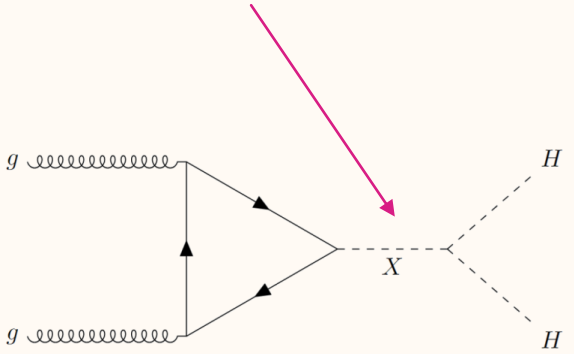

Event Selection

- preselection
  - single and dilepton triggers
  - exactly two light leptons of opposite charge ($p_T > 9\ GeV$)
  - one or two b-tagged jets ($p_T > 20\ GeV, DL1r, 77\%$)

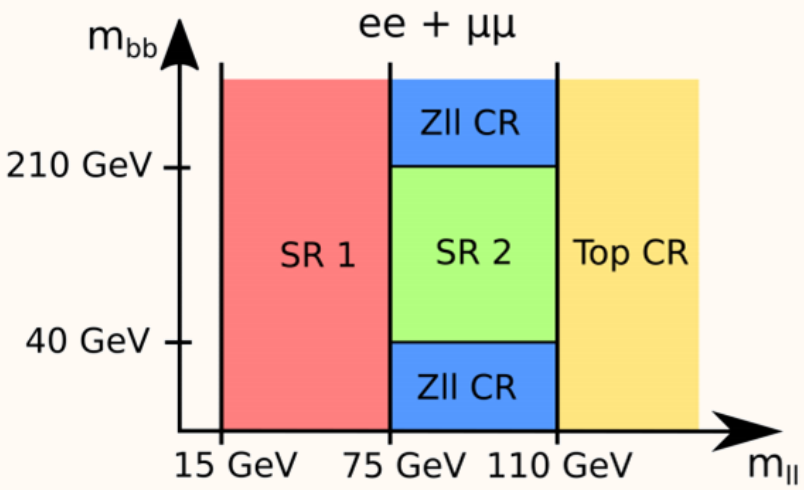

- signal region (SR) and control region (CR) split
  - SR1: target $bbWW$, $bb\tau\tau$ and low m_{ll} part of $bbZZ$
  - SR2: target high m_{ll} part of bbZZ
    - studies show that the estimated signal sensitivity in SR2 is small, so we are considering converting it into a validation region for Zll background
  - Zll CR: same definition used in $bb\tau\tau$ analysis
  - Top CR: events with high di-lepton invariant mass
    - we are considering re-defining the Top CR by using bins in the DNN score with low signal yield

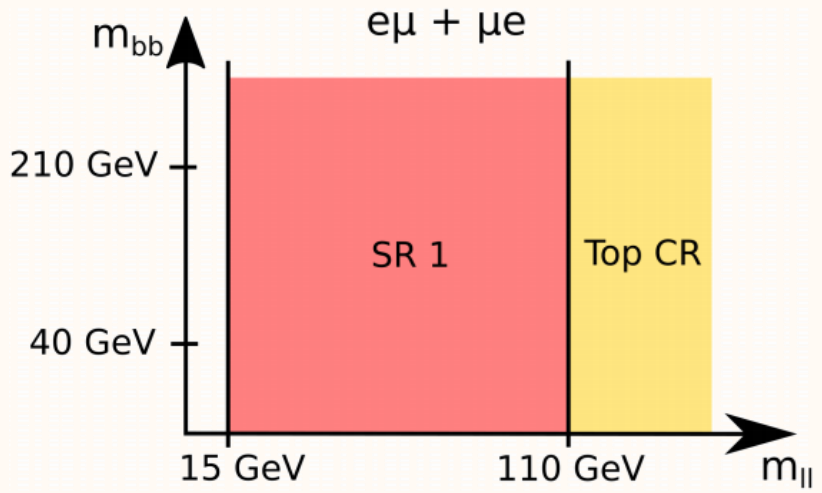

MVA Methods Overview

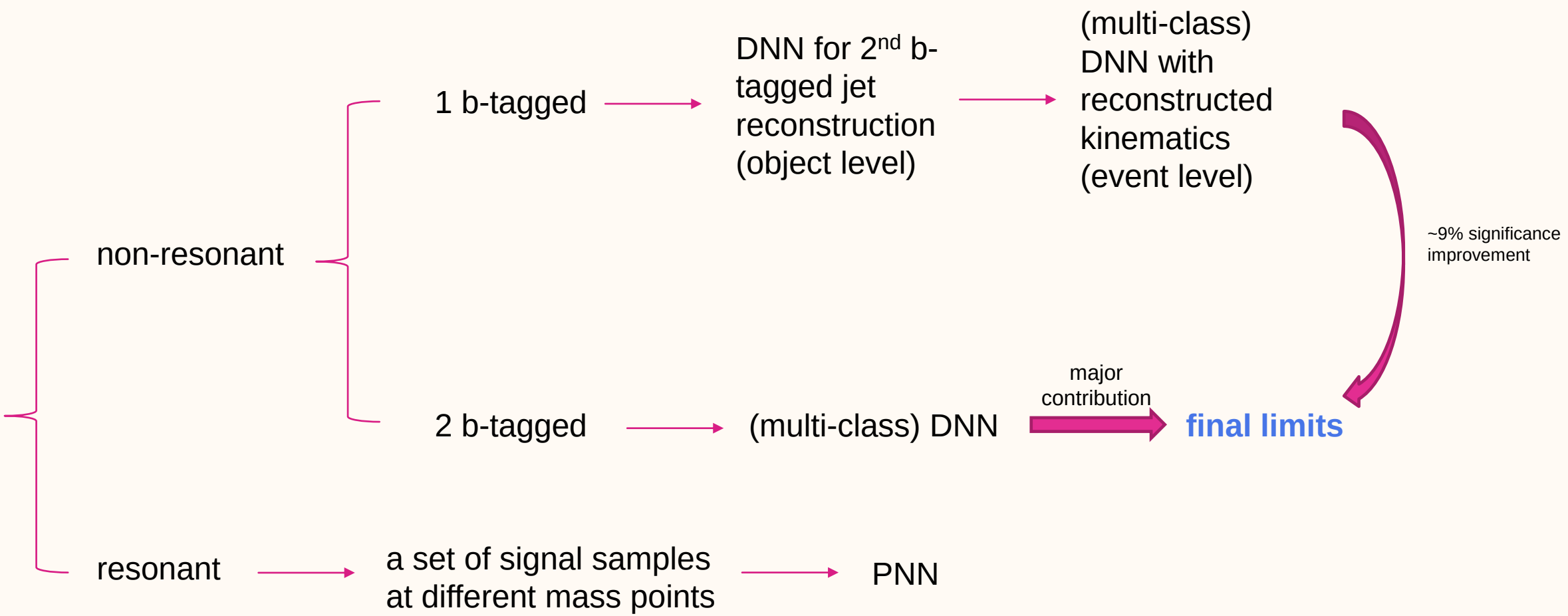

Multi-class Neural Network

- All networks are set up with 3 or 4 output classes
  - SR1: signal, top and other
  - SR2: signal, top, Zll and other

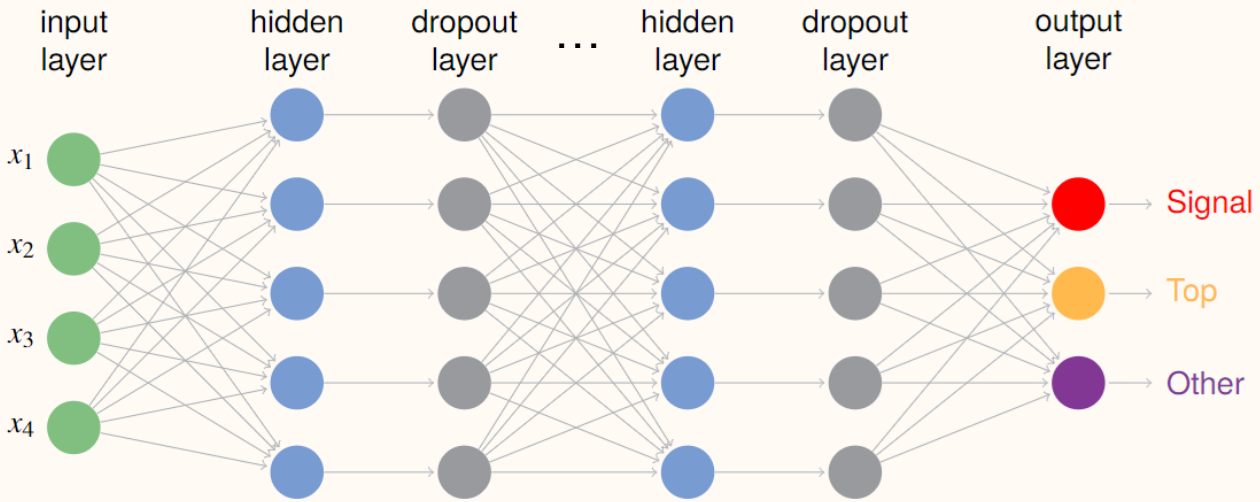

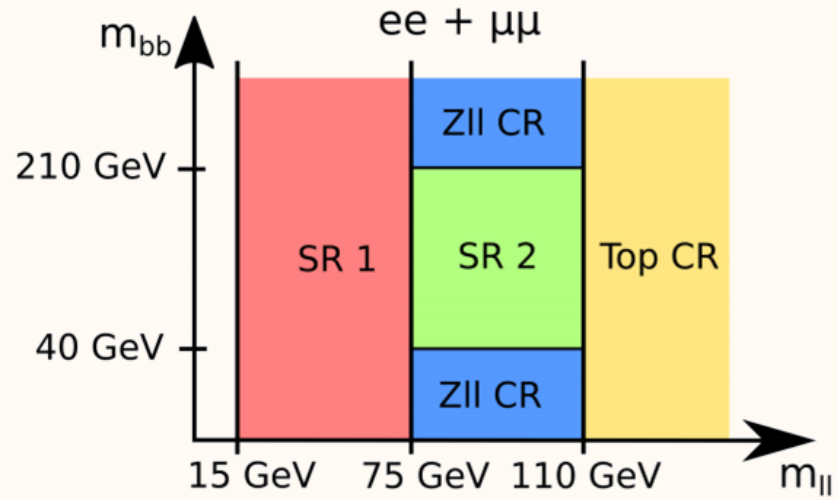

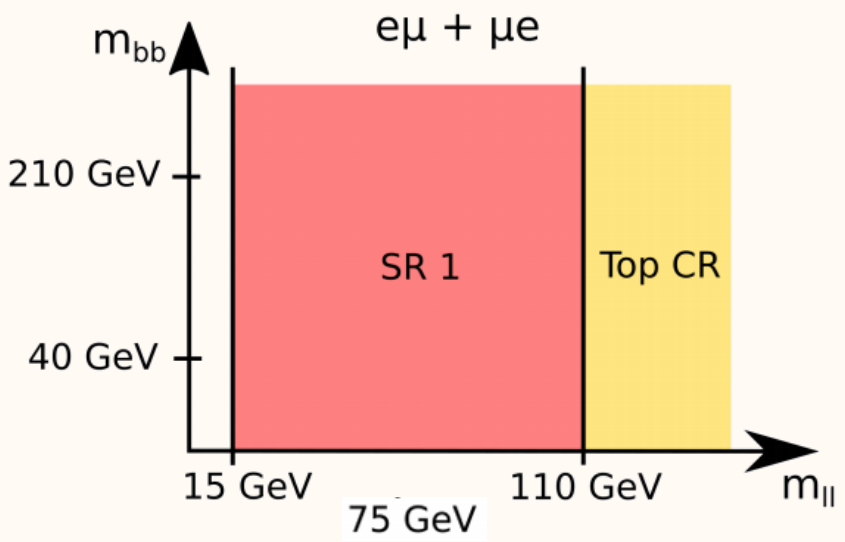

Score distribution

SR1

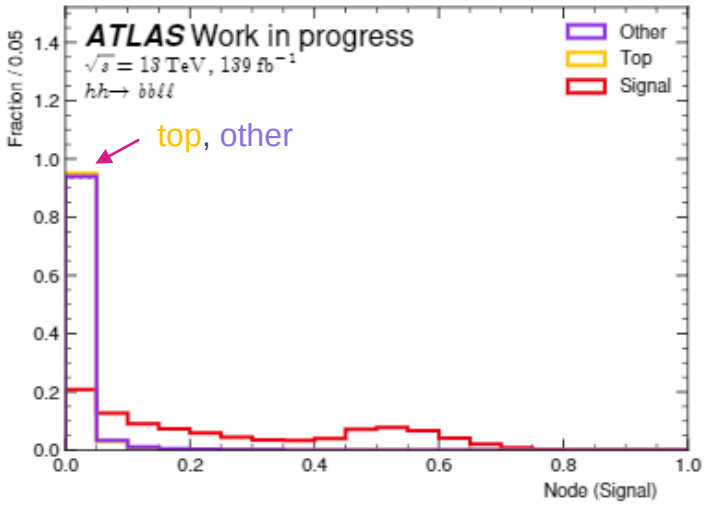

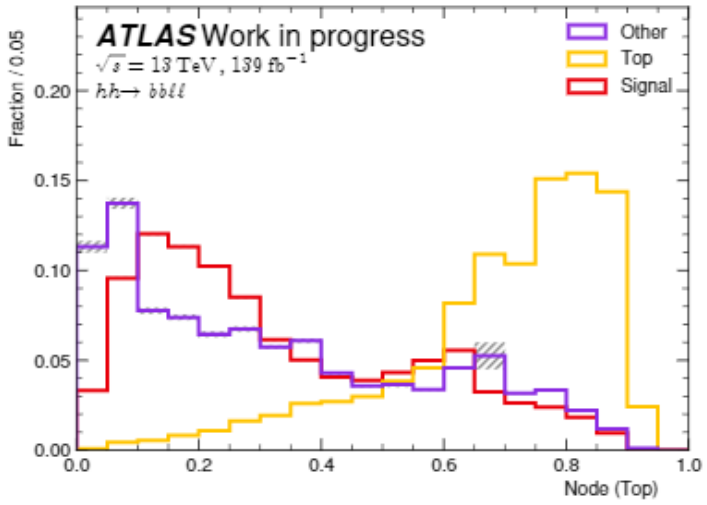

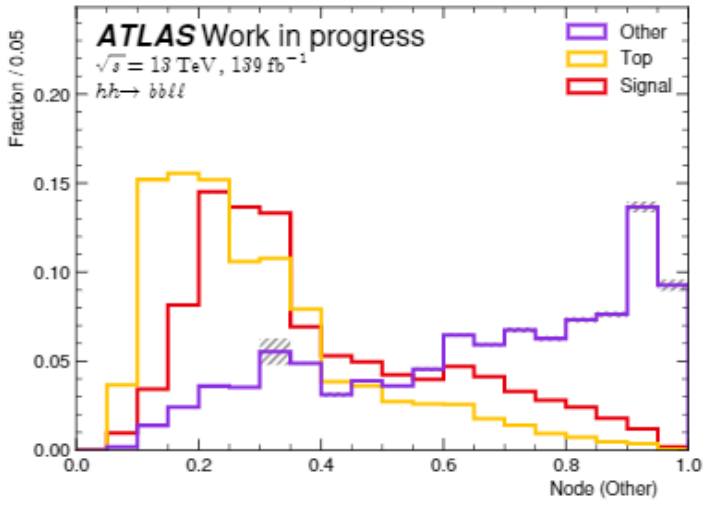

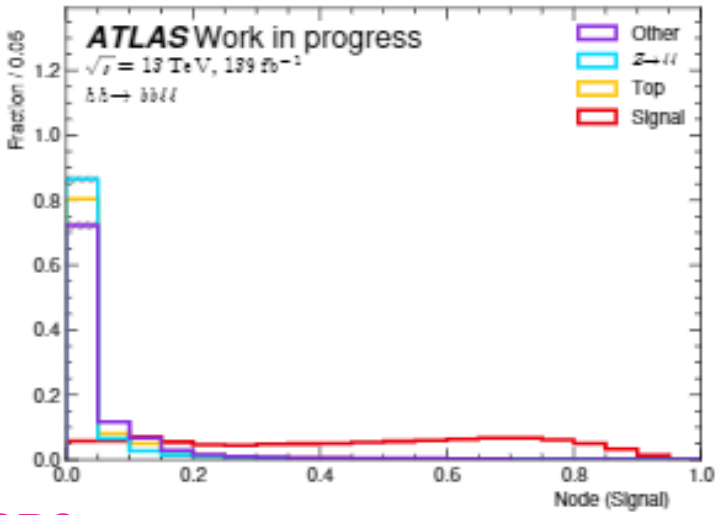

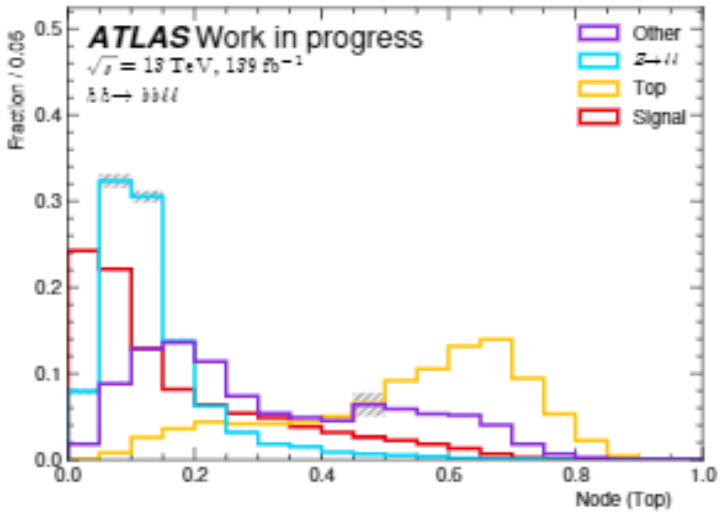

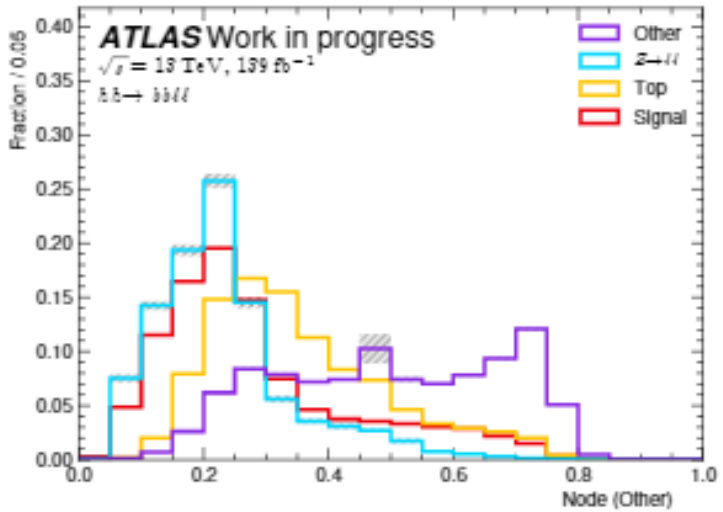

SR2

Second b-tag jet selection in 1 b-tagged Region

- To perform the same MVA training strategy in 1 b-tag region, we need to select the second b-tag jet candidate from the jets that were not tagged as b jet
  - train an object level classifier to pick the second b-tag jet
- For training, we train the correct second b-tag jets' kinematics versus incorrect second b-tag jets' kinematics
  - the correct second b-tag jets are selected with truth-information
  - the inputs and the classifier output scores are shown below

single jet	p_T, η, ϕ
jet pair	$p_T, \eta, \phi, m, \Delta\eta, \Delta\phi$
p_T rank	highest p_T ordering
$m_l l$ match	best $m_l l$ match after pairing with the first b-tag jet
p_T pair ordering	highest p_T after pairing with the first b-tag jet

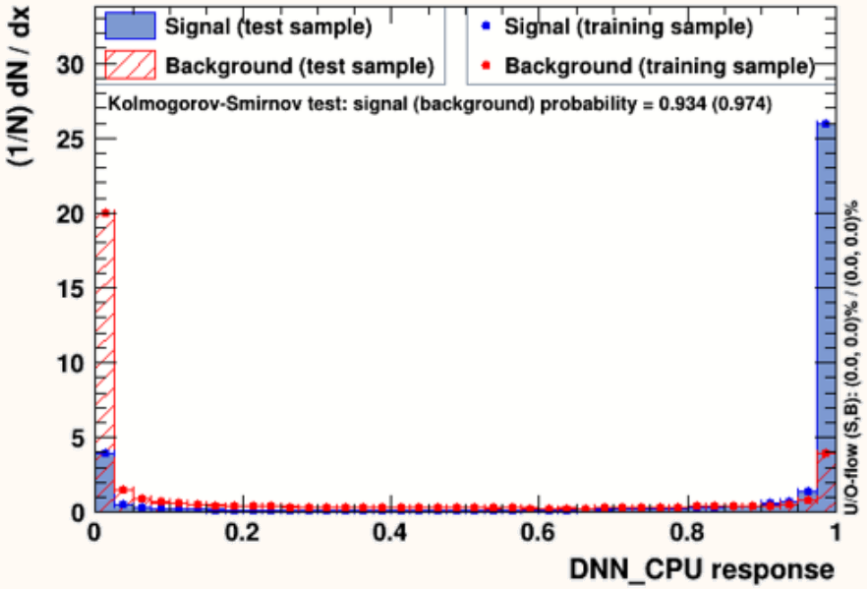

Scores Distribution in 1-btag-region

same flavor lepton pair

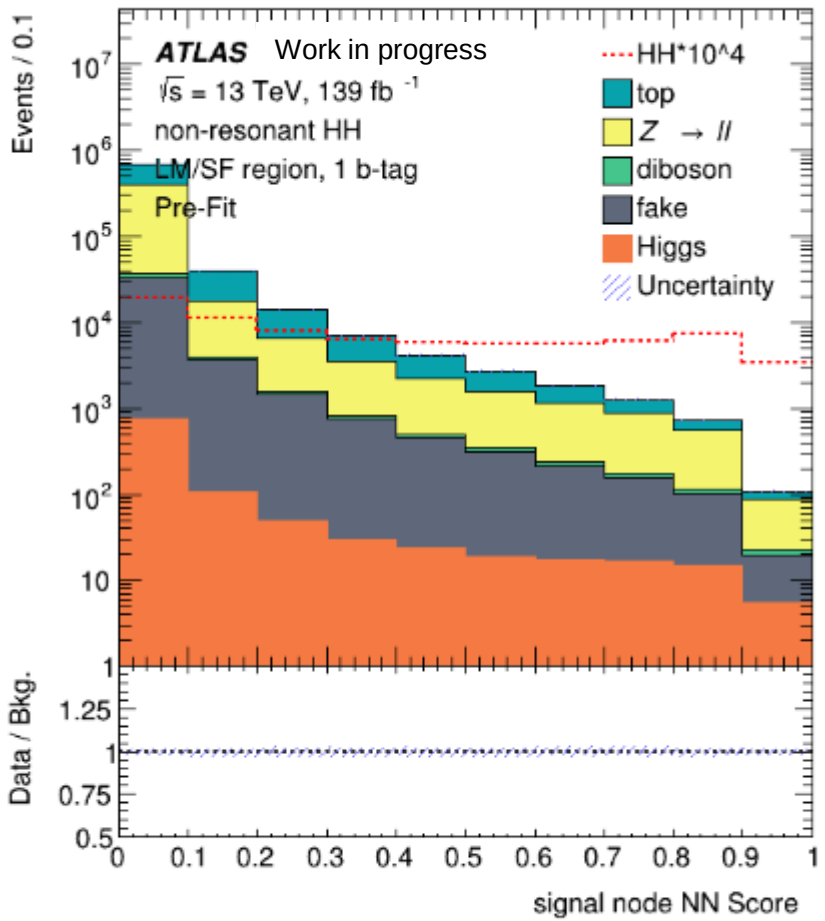

different flavor lepton pair

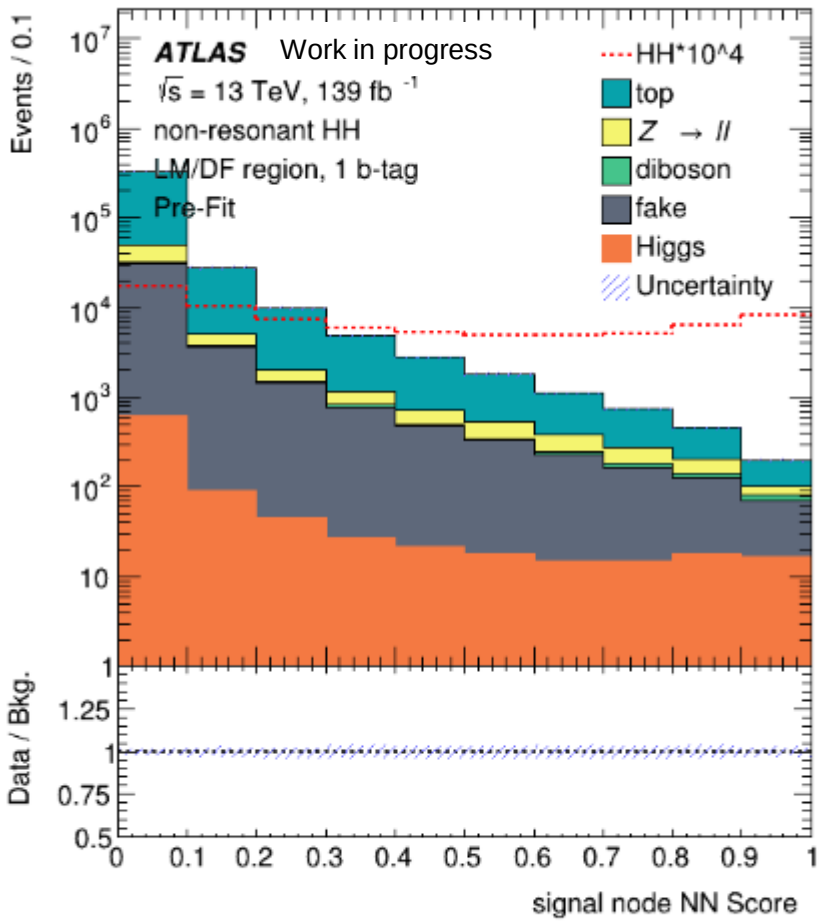

Figure 13: DNN score distribution in 1 b-tag region with systematic uncertainties included

pDNN for Resonant Search

- pDNN (parameterized Deep Neural Network)
  - Supervised training with labeled mixture of inputs
    - measured features (x_i) + physic para. (θ)
  - Smoothly interpolation between given mass points
    - single NN (neural network) work at all given mass points and in-between (suppose no dramatic kinematics change between adjacent mass points)
- We have a set of different signal samples at different mass points, which makes pDNN suitable for the resonant study
- Reference paper
  - arXiv:1601.07913

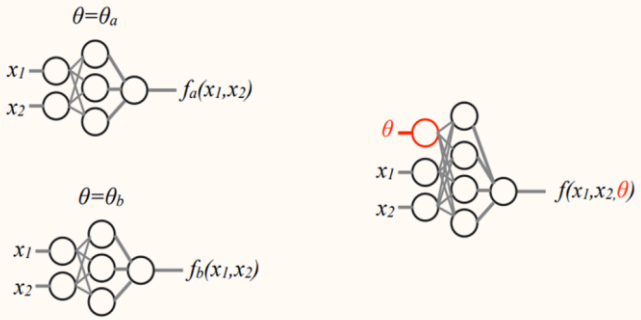

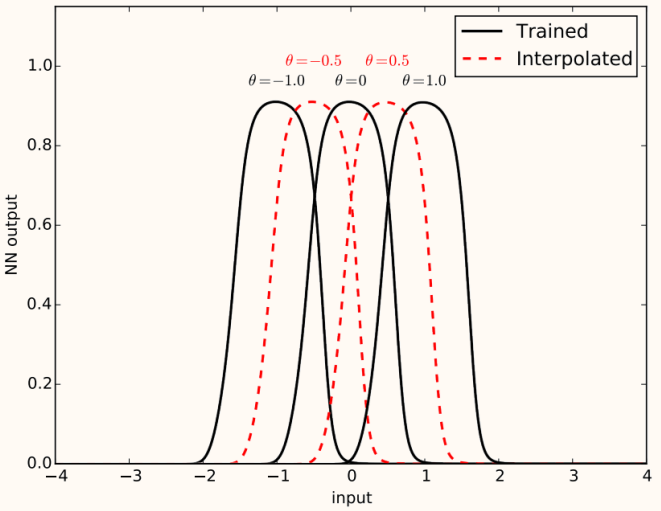

Preliminary limits (blinded)

non-resonant

Table 33: Observed and expected upper limits on the ggF-initiated non-resonant HH production cross-section at 95% CL and their ratios to the SM prediction ($\sigma^{\mathrm{SM}}(gg \to HH) = 31.05 \pm 1.90$ fb [67–73]). The $\pm 1\sigma$ and $\pm 2\sigma$ variations about the expected limit are also shown. The errors include all of the experimental and theory systematics as described in Section 7.4.

	-2σ	-1σ	**Expected**	$+1\sigma$	$+2\sigma$	**Observed**
$\sigma\,(gg \to HH)$ [fb]	228	308	429	595	798	blinded
$\sigma\,(gg \to HH)\,/\sigma^{\mathrm{SM}}\,(gg \to HH)$	7.4	9.9	13.8	19.2	25.7	blinded

resonant

mass	251	260	300	400	500	600	800	1000
Stats only	1.079	1.713	2.498	0.8655	0.2363	0.1141	0.0542	0.03689
Theo	1.080	1.715	2.523	0.8698	0.2378	0.1149	0.0545	0.03709
Theo + sys	1.479	2.797	4.041	1.647	0.2845	0.1175	0.0551	0.03731

limits set on cross section of $m_X \to HH$ (unit: pb)

Summary

- Presented the analysis for $HH \rightarrow bblvlv$ with the full Run 2 data
- For the preliminary results, we set the expected limits for:
  - non-resonant: $429\ fb$ (13.8 times of the SM)
  - resonant: $\sim 37 - 2523\ fb$ (for mass between 251 and 1000 GeV)

Backups

Background Estimation

- Dominant backgrounds
  - $t\bar{t}/Wt/t\bar{t}V$: 94% (SR1)
  - $Z \rightarrow ll$ and fakes: 3% each (SR1)
  - ttbar and Zll normalization constrained from top and Zll CRs
- Fake lepton background
  - currently estimated from Monte Carlo (MC)
- Other backgrounds
  - Ztautau, W+jets, diboson, single-Higgs (ttH, WH, ZH, ggH, VBF)
  - Estimated from MC

Trigger List

Type	Year	Trigger	p_{T}^{0} [GeV]	p_{T}^{1} [GeV]
single electron	2015	HLT_e24_lhmedium_L1EM20VH, HLT_e60_lhmedium, HLT_e120_lhloose	25	–
	2016-2018	HLT_e26_lhtight_nod0_ivarloose, HLT_e60_lhmedium_nod0, HLT_e140_lhloose_nod0	27	–
single muon	2015	HLT_mu20_iloose_L1MU15, HLT_mu50	21	–
	2016-2018	HLT_mu26_ivarmedium, HLT_mu50	28	–
di-electron	2015	HLT_2e12_lhloose_L12EM10VH	13	13
	2016	HLT_2e17_lhvloose_nod0	18	18
	2017	HLT_2e24_lhvloose_nod0 (only for period B5-B8)	25	25
	2017/2018	HLT_2e17_lhvloose_nod0_L12EM15VHI, HLT_2e24_lhvloose_nod0 (not for period 2017 B5-B8)	18	18
di-muon	2015	HLT_mu18_mu8noL1	19	10
	2016-2018	HLT_mu22_mu8noL1	24	10
electron-muon	2015	HLT_e17_lhloose_mu14	18	15
	2016-2018	HLT_e17_lhloose_nod0_mu14	18	15
	2016	HLT_e26_lhmedium_nod0_L1EM22VHI_mu8noL1 ($e\mu$ only)	27	9
	2017-2018	HLT_e26_lhmedium_nod0_mu8noL1 ($e\mu$ only)	27	9
	2015	HLT_e7_lhmedium_mu24 (μe only)	26	9
	2016-2018	HLT_e7_lhmedium_nod0_mu24 (μe only)	26	9

- for each year, a logical “OR” is performed between all triggers to select events
- offline p_T threshold
  - electrons: $p_T^{offline} \geq p_T^{trigger} + 1\ GeV$
  - muons: $p_T^{offline} \geq 1.05 \times p_T^{trigger}$ (round to next higher integer)

Signal Samples

I.1.1 Non-resonant ggF, NLO+FT

$\kappa_\lambda = 1$

mc16_13TeV.600047.PhH7EG_PDF4LHC15_HHbbWW2L_cHHH01d0.deriv.DAOD_SUSY2.e7954_s3126_r9364_p3990

mc16_13TeV.600045.PhH7EG_PDF4LHC15_HHbbtt2L_cHHH01d0.deriv.DAOD_SUSY2.e7954_s3126_r9364_p3990

mc16_13TeV.600049.PhH7EG_PDF4LHC15_HHbbZZ2L_cHHH01d0.deriv.DAOD_SUSY2.e7954_s3126_r9364_p3990

$\kappa_\lambda = 10$

mc16_13TeV.600048.PhH7EG_PDF4LHC15_HHbbWW2L_cHHH10d0.deriv.DAOD_SUSY2.e7954_s3126_r9364_p3990

mc16_13TeV.600046.PhH7EG_PDF4LHC15_HHbbtt2L_cHHH10d0.deriv.DAOD_SUSY2.e7954_s3126_r9364_p3990

mc16_13TeV.600050.PhH7EG_PDF4LHC15_HHbbZZ2L_cHHH10d0.deriv.DAOD_SUSY2.e7954_s3126_r9364_p3990

I.1.2 Resonant ggF

mc16_13TeV.450624.MadGraphHerwig7EvtGen_NNPDF23LO_X251tohh_WWbb_2lep.deriv.DAOD_SUSY2.e7453_a875_r9364_p3990

mc16_13TeV.450625.MadGraphHerwig7EvtGen_NNPDF23LO_X260tohh_WWbb_2lep.deriv.DAOD_SUSY2.e7453_a875_r9364_p3990

mc16_13TeV.450626.MadGraphHerwig7EvtGen_NNPDF23LO_X300tohh_WWbb_2lep.deriv.DAOD_SUSY2.e7453_a875_r9364_p3990

mc16_13TeV.450627.MadGraphHerwig7EvtGen_NNPDF23LO_X400tohh_WWbb_2lep.deriv.DAOD_SUSY2.e7453_a875_r9364_p3990

mc16_13TeV.450628.MadGraphHerwig7EvtGen_NNPDF23LO_X500tohh_WWbb_2lep.deriv.DAOD_SUSY2.e7453_a875_r9364_p3990

mc16_13TeV.450629.MadGraphHerwig7EvtGen_NNPDF23LO_X600tohh_WWbb_2lep.deriv.DAOD_SUSY2.e7453_a875_r9364_p3990

mc16_13TeV.450630.MadGraphHerwig7EvtGen_NNPDF23LO_X800tohh_WWbb_2lep.deriv.DAOD_SUSY2.e7453_a875_r9364_p3990

mc16_13TeV.450631.MadGraphHerwig7EvtGen_NNPDF23LO_X1000tohh_WWbb_2lep.deriv.DAOD_SUSY2.e7453_a875_r9364_p3990

mc16_13TeV.450652.MadGraphHerwig7EvtGen_NNPDF23LO_X251tohh_bbZZllvv.deriv.DAOD_SUSY2.e7452_a875_r9364_p3990

mc16_13TeV.450653.MadGraphHerwig7EvtGen_NNPDF23LO_X260tohh_bbZZllvv.deriv.DAOD_SUSY2.e7452_a875_r9364_p3990

mc16_13TeV.450654.MadGraphHerwig7EvtGen_NNPDF23LO_X300tohh_bbZZllvv.deriv.DAOD_SUSY2.e7452_a875_r9364_p3990

mc16_13TeV.450655.MadGraphHerwig7EvtGen_NNPDF23LO_X400tohh_bbZZllvv.deriv.DAOD_SUSY2.e7452_a875_r9364_p3990

mc16_13TeV.450656.MadGraphHerwig7EvtGen_NNPDF23LO_X500tohh_bbZZllvv.deriv.DAOD_SUSY2.e7452_a875_r9364_p3990

mc16_13TeV.450657.MadGraphHerwig7EvtGen_NNPDF23LO_X600tohh_bbZZllvv.deriv.DAOD_SUSY2.e7452_a875_r9364_p3990

mc16_13TeV.450658.MadGraphHerwig7EvtGen_NNPDF23LO_X800tohh_bbZZllvv.deriv.DAOD_SUSY2.e7452_a875_r9364_p3990

mc16_13TeV.450659.MadGraphHerwig7EvtGen_NNPDF23LO_X1000tohh_bbZZllvv.deriv.DAOD_SUSY2.e7452_a875_r9364_p3990

mc16_13TeV.451708.MadGraphHerwig7EvtGen_NNPDF23LO_X251tohh_ttbb_2lep.deriv.DAOD_SUSY2.e8091_a875_r9364_p3990

mc16_13TeV.451709.MadGraphHerwig7EvtGen_NNPDF23LO_X260tohh_ttbb_2lep.deriv.DAOD_SUSY2.e8091_a875_r9364_p3990

mc16_13TeV.451710.MadGraphHerwig7EvtGen_NNPDF23LO_X300tohh_ttbb_2lep.deriv.DAOD_SUSY2.e8091_a875_r9364_p3990

mc16_13TeV.451711.MadGraphHerwig7EvtGen_NNPDF23LO_X400tohh_ttbb_2lep.deriv.DAOD_SUSY2.e8091_a875_r9364_p3990

mc16_13TeV.451712.MadGraphHerwig7EvtGen_NNPDF23LO_X500tohh_ttbb_2lep.deriv.DAOD_SUSY2.e8091_a875_r9364_p3990

mc16_13TeV.451713.MadGraphHerwig7EvtGen_NNPDF23LO_X600tohh_ttbb_2lep.deriv.DAOD_SUSY2.e8091_a875_r9364_p3990

mc16_13TeV.451714.MadGraphHerwig7EvtGen_NNPDF23LO_X800tohh_ttbb_2lep.deriv.DAOD_SUSY2.e8091_a875_r9364_p3990

mc16_13TeV.451715.MadGraphHerwig7EvtGen_NNPDF23LO_X1000tohh_ttbb_2lep.deriv.DAOD_SUSY2.e8091_a875_r9364_p3990

Event yields

Work in progress

Process	SR1	SR1 SF	SR1 DF	SR2	TopCR	ZllCR
			SM background			
$t\bar{t}$	602330 ± 170	231930 ± 100	370400 ± 130	105810 ± 70	428860 ± 140	33500 ± 40
Wt	17310 ± 50	6450 ± 29	10860 ± 40	3135 ± 21	16880 ± 50	1213 ± 13
$t\bar{t}+V$	1345 ± 5	573.5 ± 3.0	771 ± 4	909.8 ± 2.8	1235 ± 5	435.4 ± 1.9
$Z \to ee$	7670 ± 150	7630 ± 150	38 ± 7	60510 ± 340	2100 ± 70	19950 ± 160
$Z \to \mu\mu$	12210 ± 190	12160 ± 190	54 ± 9	82400 ± 400	2670 ± 70	26510 ± 220
$Z \to \tau\tau$	2760 ± 70	1360 ± 50	1400 ± 50	41 ± 11	13 ± 6	9.8 ± 3.4
Diboson	475 ± 5	328 ± 4	147.2 ± 2.3	4671 ± 15	240.7 ± 3.2	408 ± 5
Higgs	799 ± 4	378.1 ± 3.5	420.9 ± 2.7	1676 ± 12	391.1 ± 2.6	63.5 ± 1.7
Fakes	18930 ± 110	7790 ± 80	11140 ± 70	2627 ± 27	7630 ± 40	716 ± 10
Total SM bkg.	663830 ± 330	268600 ± 280	395230 ± 160	261800 ± 500	460010 ± 190	82810 ± 280
			Non-resonant signal, ggF			
ggF $HH \to bbWW$	9.088 ± 0.017	4.523 ± 0.012	4.565 ± 0.012	0.0563 ± 0.0013	0.00145 ± 0.00021	0.00129 ± 0.00019
ggF $HH \to bb\tau\tau$	3.433 ± 0.009	1.598 ± 0.006	1.835 ± 0.007	0.2362 ± 0.0025	0.00394 ± 0.00032	0.00450 ± 0.00035
ggF $HH \to bbZZ$	0.2246 ± 0.0009	0.2202 ± 0.0009	0.00435 ± 0.00013	0.3225 ± 0.0011	0.000146 ± 0.000024	0.00704 ± 0.00017
Σ ggF HH	12.745 ± 0.019	6.341 ± 0.014	6.404 ± 0.014	0.6149 ± 0.0030	0.0055 ± 0.0004	0.0128 ± 0.0004
			Non-resonant signal, VBF			
VBF $HH \to bbWW$	0.3621 ± 0.0022	0.1796 ± 0.0015	0.1825 ± 0.0016	0.00213 ± 0.00017	0.00013 ± 0.00004	0.000067 ± 0.000030
VBF $HH \to bb\tau\tau$	0.1294 ± 0.0009	0.0600 ± 0.0006	0.0694 ± 0.0007	0.01023 ± 0.00026	0.000133 ± 0.000029	0.00023 ± 0.00004
VBF $HH \to bbZZ$	0.00804 ± 0.00008	0.00790 ± 0.00008	0.000147 ± 0.000011	0.01351 ± 0.00011	0.0000106 ± 0.0000031	0.000340 ± 0.000017
Σ VBF HH	0.4995 ± 0.0024	0.2476 ± 0.0017	0.2520 ± 0.0017	0.02587 ± 0.00032	0.00028 ± 0.00005	0.00063 ± 0.00005
			Non-resonant signal, ggF+VBF			
Σ ggF+VBF HH	13.245 ± 0.019	6.588 ± 0.014	6.656 ± 0.014	0.6408 ± 0.0030	0.0058 ± 0.0004	0.0135 ± 0.0004

Table 6: Yields for SM background processes and non-resonant SM ggF and VBF signals in the bbll regions defined in Section 4.2.

m_{ll} Distribution After the Preselection

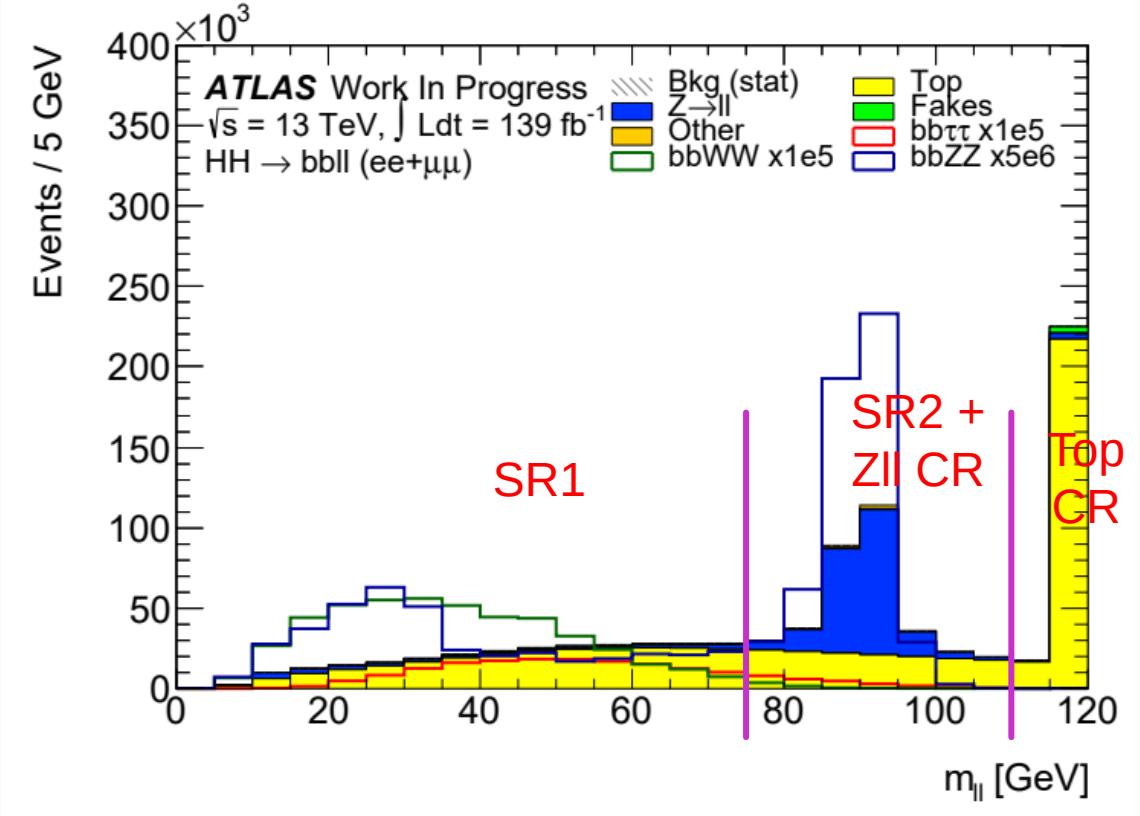

same flavor

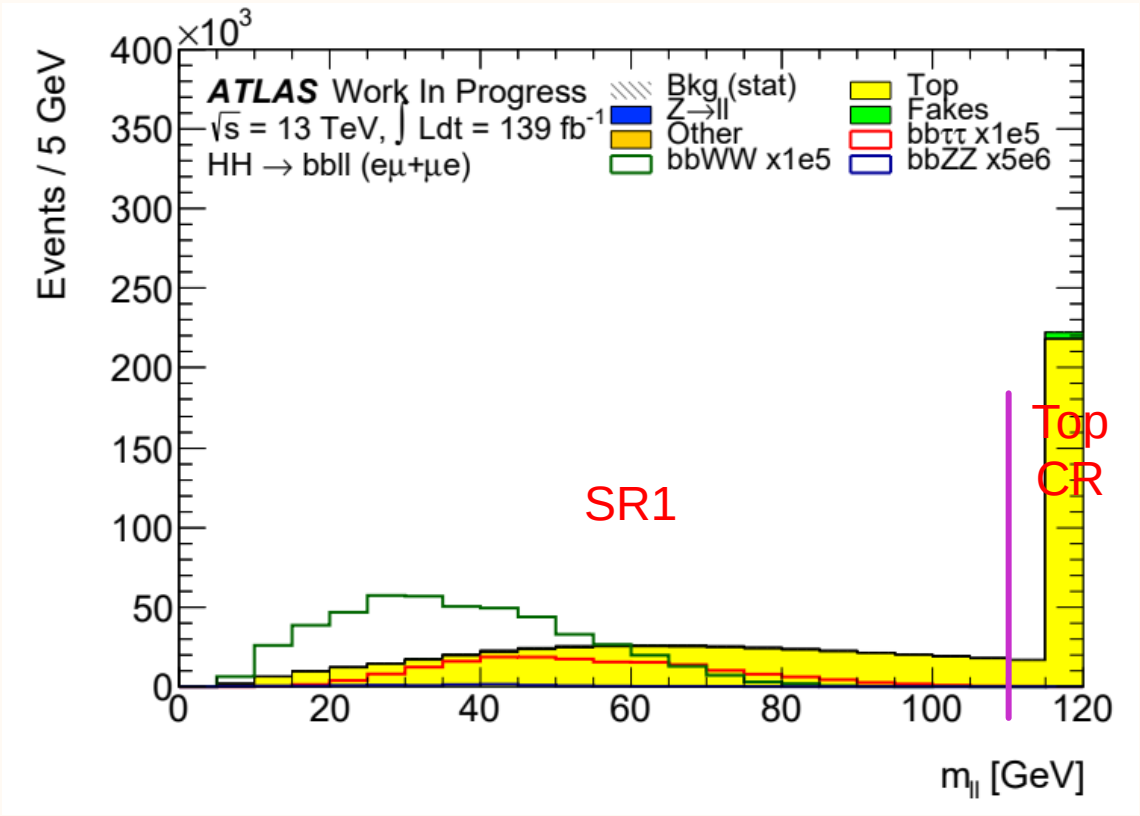

different flavor

m_{ll} Distribution After the Preselection

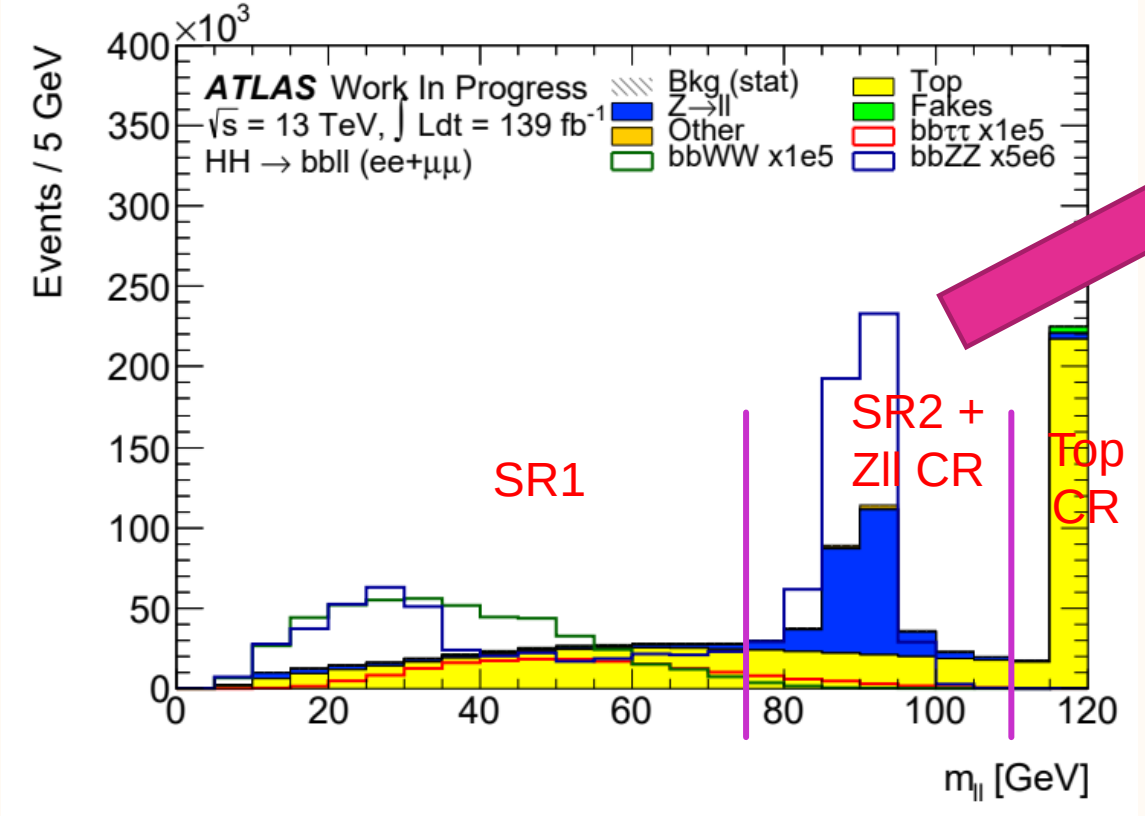

same flavor

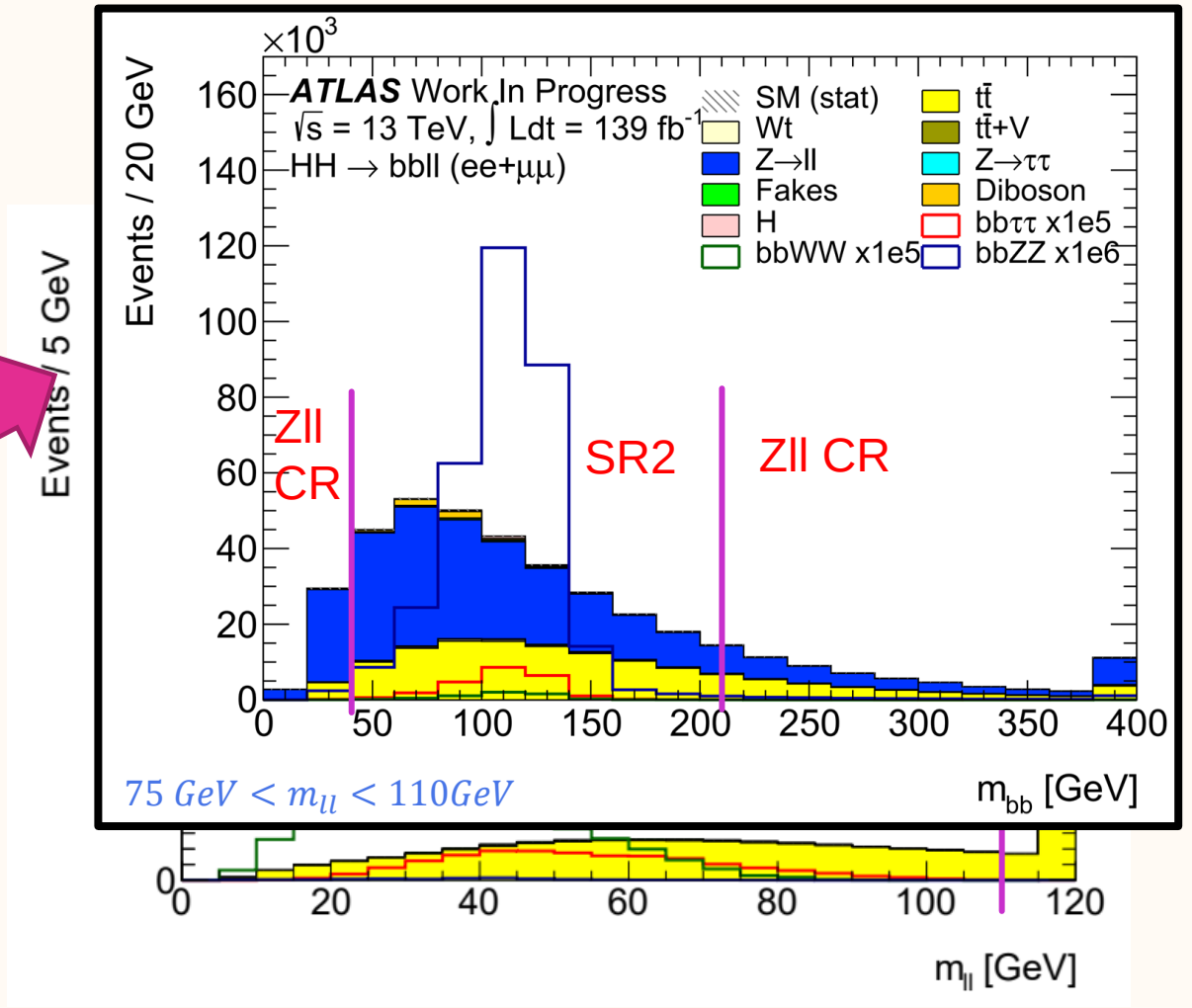

different flavor

m_{ll} Distribution in SR1

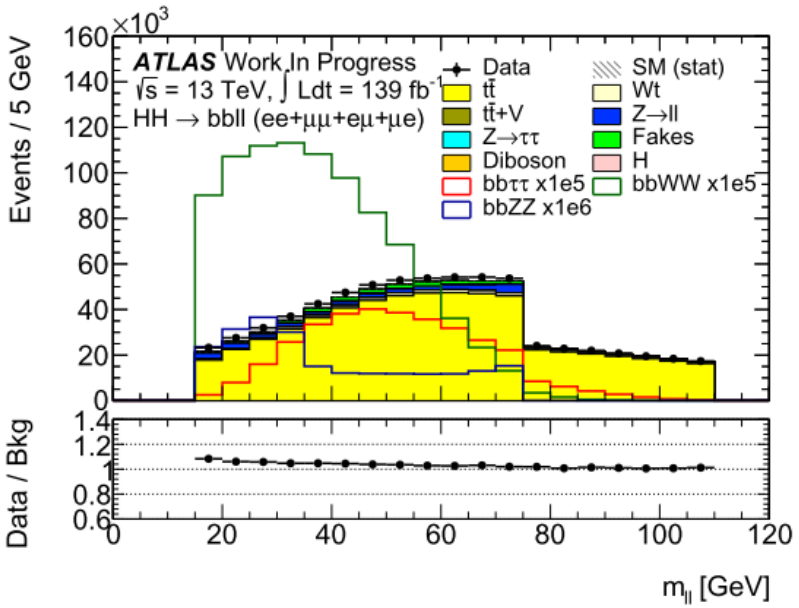

inclusive

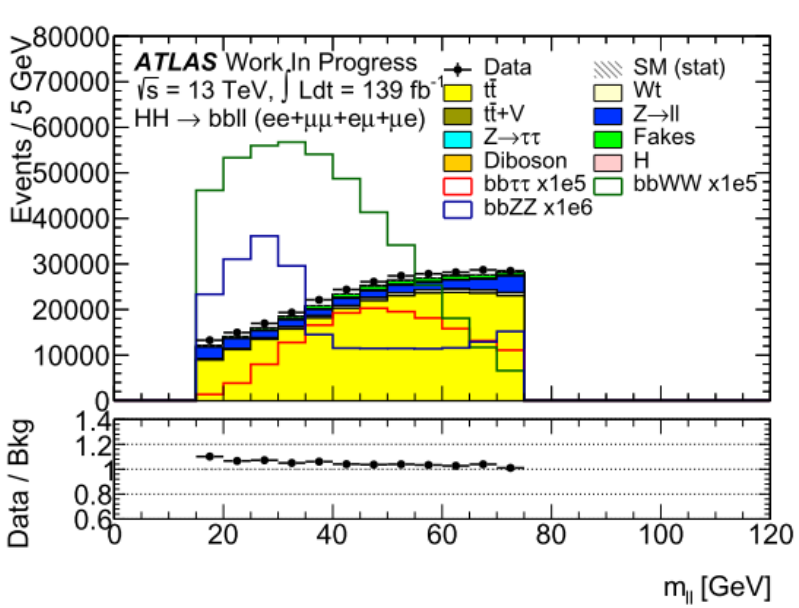

same-flavor

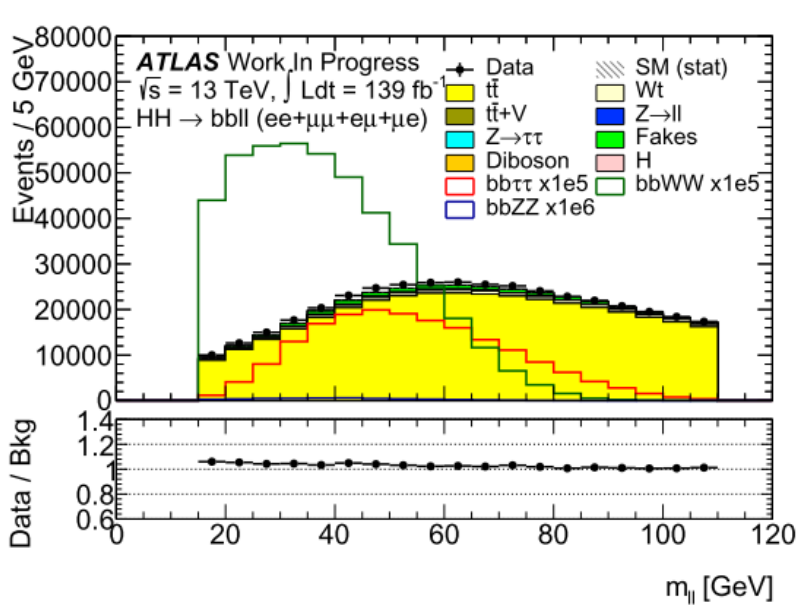

different-flavor

Weight Systematics

- Electrons
  - ATLAS_EL_EFF_TRIG_TOTAL_1NPCOR_PLUS_UNCOR
  - ATLAS_EL_EFF_RECO_TOTAL_1NPCOR_PLUS_UNCOR
  - ATLAS_EL_EFF_ID_TOTAL_1NPCOR_PLUS_UNCOR
  - ATLAS_EL_EFF_ISO_TOTAL_1NPCOR_PLUS_UNCOR
- Muons
  - ATLAS_MUON_EFF_TrigStatUncertainty
  - ATLAS_MUON_EFF_TrigSystUncertainty
  - ATLAS_MUON_EFF_RECO_STAT
  - ATLAS_MUON_EFF_RECO_SYS
  - ATLAS_MUON_EFF_RECO_STAT_LOWPT
  - ATLAS_MUON_EFF_RECO_SYS_LOWPT
  - ATLAS_MUON_EFF_ISO_STAT
  - ATLAS_MUON_EFF_ISO_SYS
- Jets
  - ATLAS_JET_JVT_EFF
  - ATLAS_JET_FJVT_EFF
- Pileup
  - ATLAS_PU_PRW_DATASF
- Flavor tagging
  - ATLAS_FT_EFF_Eigen_B_0
  - ATLAS_FT_EFF_Eigen_B_1
  - ATLAS_FT_EFF_Eigen_B_2
  - ATLAS_FT_EFF_Eigen_B_3
  - ATLAS_FT_EFF_Eigen_B_4
  - ATLAS_FT_EFF_Eigen_B_5
  - ATLAS_FT_EFF_Eigen_B_6
  - ATLAS_FT_EFF_Eigen_B_7
  - ATLAS_FT_EFF_Eigen_B_8
  - ATLAS_FT_EFF_Eigen_C_0
  - ATLAS_FT_EFF_Eigen_C_1
  - ATLAS_FT_EFF_Eigen_C_2
  - ATLAS_FT_EFF_Eigen_C_3
  - ATLAS_FT_EFF_Eigen_Light_1
  - ATLAS_FT_EFF_Eigen_Light_2
  - ATLAS_FT_EFF_Eigen_Light_3
  - ATLAS_FT_EFF_extrapolation
  - ATLAS_FT_EFF_extrapolation_from_charm

Kinematic Systematics

- Electrons
  - ATLAS_EG_RESOLUTION_ALL
  - ATLAS_EG_SCALE_ALL (also apply to fastsim samples?)
  - ATLAS_EG_SCALE_AF2
- Muons
  - ATLAS_MUON_ID
  - ATLAS_MUON_MS
  - ATLAS_MUON_SCALE
  - ATLAS_MUON_SAGITTA_RHO
  - ATLAS_MUON_SAGITTA_RESBIAS
- MET
  - ATLAS_MET_SoftTrk_ResoPara (one-sided)
  - ATLAS_MET_SoftTrk_ResoPerp (one-sided)
  - ATLAS_MET_SoftTrk_ScaleUp (one-sided)
  - ATLAS_MET_SoftTrk_ScaleDown (one-sided)
- Jets
  - ATLAS_JET_EtaIntercalibration_Modelling
  - ATLAS_JET_EtaIntercalibration_TotalStat
  - ATLAS_JET_EtaIntercalibration_NonClosure_highE
  - ATLAS_JET_EtaIntercalibration_NonClosure_negEta
  - ATLAS_JET_EtaIntercalibration_NonClosure_posEta
  - ATLAS_JET_Pileup_OffsetMu
  - ATLAS_JET_Pileup_OffsetNPV
  - ATLAS_JET_Pileup_PtTerm
  - ATLAS_JET_Pileup_RhoTopology
  - ATLAS_JET_Flavor_Composition
  - ATLAS_JET_Flavor_Response
  - ATLAS_JET_PunchThrough_MC16
  - ATLAS_JET_PunchThrough_AFII
  - ATLAS_JET_EffectiveNP_Detector1
  - ATLAS_JET_EffectiveNP_Detector2
  - ATLAS_JET_EffectiveNP_Mixed1
  - ATLAS_JET_EffectiveNP_Mixed2
  - ATLAS_JET_EffectiveNP_Mixed3
  - ATLAS_JET_EffectiveNP_Modelling1
  - ATLAS_JET_EffectiveNP_Modelling2
  - ATLAS_JET_EffectiveNP_Modelling3
  - ATLAS_JET_EffectiveNP_Modelling4
  - ATLAS_JET_EffectiveNP_Statistical1
  - ATLAS_JET_EffectiveNP_Statistical2
  - ATLAS_JET_EffectiveNP_Statistical3
  - ATLAS_JET_EffectiveNP_Statistical4
  - ATLAS_JET_EffectiveNP_Statistical5
  - ATLAS_JET_EffectiveNP_Statistical6
  - ATLAS_JET_SingleParticle_HighPt
  - ATLAS_JET_RelativeNonClosure_MC16
  - ATLAS_JET_RelativeNonClosure_AFII
  - ATLAS_JET_BJES_Response
  - ATLAS_JET_EtaIntercalibration_NonClosure_2018data
  - ATLAS_JET_JER_DataVsMC_AFII
  - ATLAS_JET_JER_DataVsMC_MC16
  - ATLAS_JET_JER_EffectiveNP_1
  - ATLAS_JET_JER_EffectiveNP_2
  - ATLAS_JET_JER_EffectiveNP_3
  - ATLAS_JET_JER_EffectiveNP_4
  - ATLAS_JET_JER_EffectiveNP_5
  - ATLAS_JET_JER_EffectiveNP_6
  - ATLAS_JET_JER_EffectiveNP_7
  - ATLAS_JET_JER_EffectiveNP_8
  - ATLAS_JET_JER_EffectiveNP_9
  - ATLAS_JET_JER_EffectiveNP_10
  - ATLAS_JET_JER_EffectiveNP_11
  - ATLAS_JET_JER_EffectiveNP_12restTerm

- Luminosity
  - overall variation of 1.7%

MVA Inputs Correlations

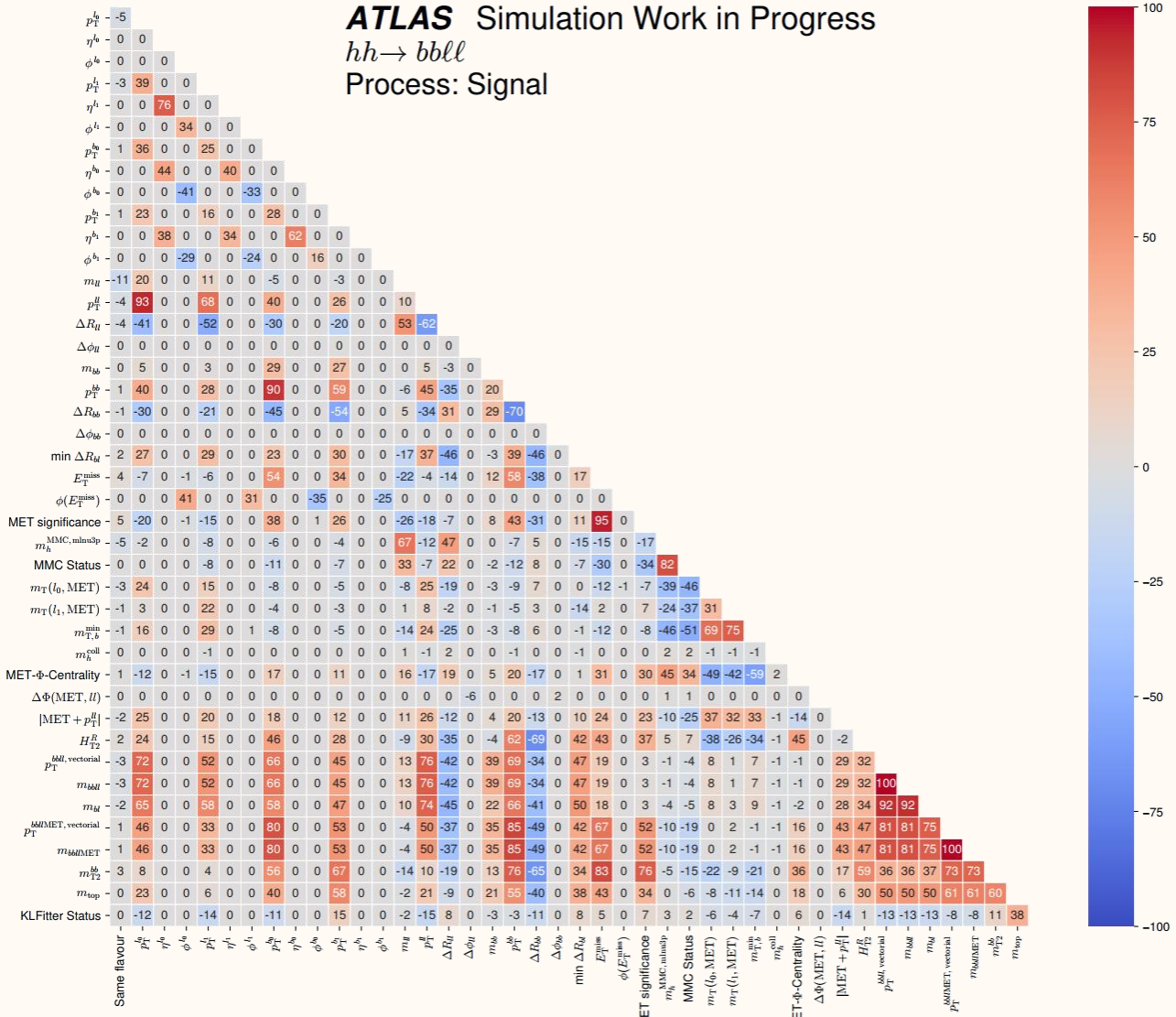

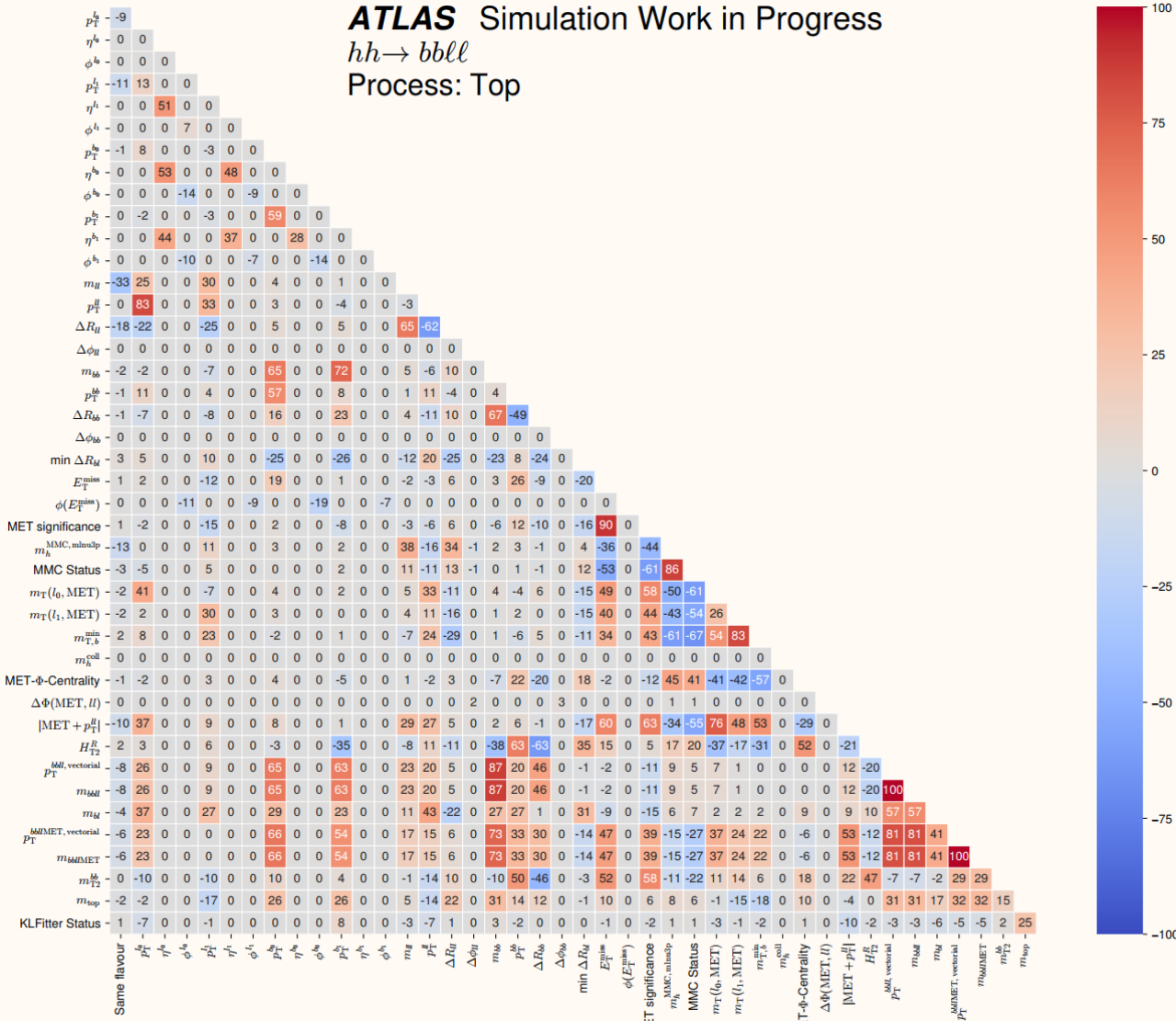

MVA Input Data Separation & Pre-Process

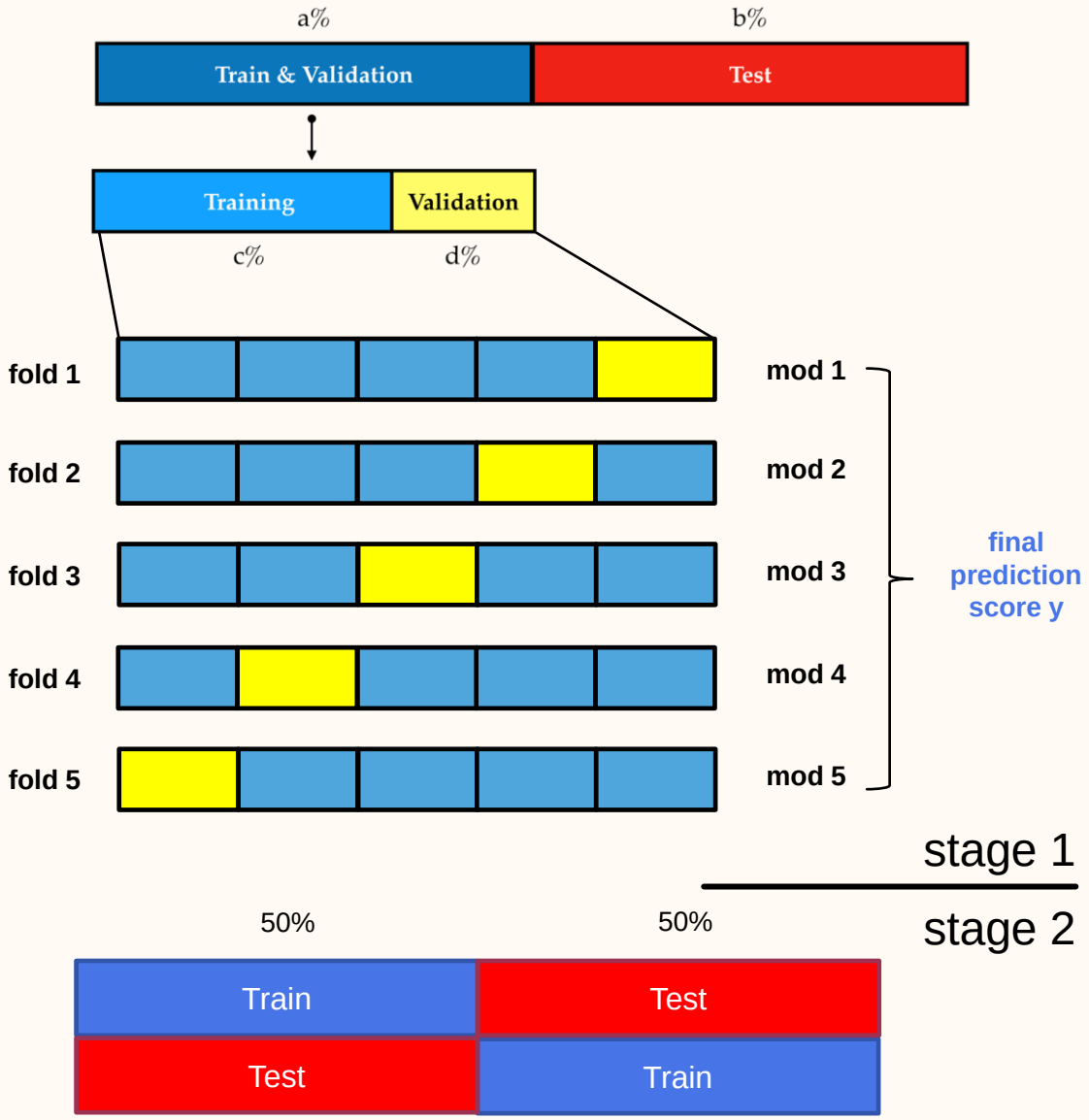

- Train & validation – test split
  - b% of input are held out to evaluate the final performance of the NN and find potential over-training issues
  - separation is “stratified” (make sure the ratio of different mc components is close in each split)
- “5-fold” train – validation split
  - a% inputs further separated to c% and d% training & validation input sets
  - can separate to 5 folds and use one-fold for validation at one time (in total perform training 5 times)
- 2-stage cross-validation
  - the best set of hyper-parameters θ_{best} selection is performed in above steps (stage 1)
  - use the θ_{best} to perform 2-fold training on full datasets

Theory Systematics - Signal

- $\mu_R + \mu_F$ scales
  - use 7-point variation: [(0.5,0.5),(0.5,1.0),(1.0,0.5),(1.0,1.0),(1.0,2.0),(2.0,1.0),(2.0,2.0)]
  - calculate envelope
- PDF variation
  - PDF4LHC15 prescription used
  - 30 internal eigen errors
  - 2 αs variations
  - 2 external variations (CT14NLO and MMHT2014nlo68clas118) → 34 variations
  - combine with Hessian method: $\Delta X = \sqrt{\sum_i (X_i - X_0)^2}$

Theory Systematics - $t\bar{t}$ & Wt

- $\mu_R + \mu_F$ scales
  - use 7-point variation: [(0.5,0.5),(0.5,1.0),(1.0,0.5),(1.0,1.0),(1.0,2.0),(2.0,1.0),(2.0,2.0)]
  - calculate envelope
- PDF
  - 30 PDF4LHC15 replicas
    - combine with Hessian method w.r.t. to central value (X_0) of PDF4LHC15 set

$$\Delta X = \sqrt{\sum_i (X_i - X_0)^2}$$

  - 2 αs variations → combine with PDF uncertainties

$$\delta^{PDF+\alpha_S} = \sqrt{(\delta^{PDF})^2 + (\delta^{\alpha_S})^2}$$

- Others
  - ISR / FSR
- Alternative samples (available in fastsim only)
  - compare with fastsim version of nominal sample (Powheg+Pythia 8)
  - matrix element: aMCatNLO+Pythia8
  - parton shower: Powheg+Herwig7
- $t\bar{t}$ & Wt interference
  - will look at the DS scheme (nominal samples uses DR scheme)

Theory Systematics - Z+Jets

- $\mu_R + \mu_F$ scales
  - use 7-point variation: [(0.5,0.5),(0.5,1.0),(1.0,0.5),(1.0,1.0),(1.0,2.0),(2.0,1.0),(2.0,2.0)]
  - calculate envelope
- PDF
  - 100 NNPDF replicas
    - combine with standard deviation (X0 is the nominal value, which is already the mean of all replicas)

$$\Delta X = \sqrt{\frac{1}{N}\sum_i (X_i - X_0)^2}$$

  - 2 αs variations
  - 2 external PDF sets (MMHT2014nnlo68cl and CT14nnlo)
- CKKW and QSF variations
- Alternative samples
  - alternative Madgraph+Pythia8 samples compared with nominal sample (Sherpa)
  - combined matrix element + parton shower uncertainty

Experimental Systematics

- Luminosity
  - overall variation of 1.7%
- Pileup
  - reweighting uncertainty
- Muon/Electron
  - trigger, identification, reconstruction, isolation, p_T scale, and resolution
- MET
  - soft term scale and resolution
- Jet
  - energy resolution/scale, η intercalibration, JVT efficiency
- Flavor tagging
  - scale of b/c/light-jets and extrapolation